

Spatial Interaction Filters for Monitoring Harmful Algae Blooms

Yang Cai

Carnegie Mellon University
Pittsburgh, PA 15213, USA
yangcai@cs.cmu.edu

Sai Ho Chung

Carnegie Mellon University
Pittsburgh, PA 15213
saic@andrew.cmu.edu

Richard Stumpf

NOAA National Ocean Service
Silver Spring, MD 20910
richard.stumpf@noaa.gov

Timothy Wynne

NOAA National Ocean Service
Silver Spring, MD 20910
timothy.wynne@noaa.gov

Michelle Tomlinson

NOAA National Ocean Service
Silver Spring, MD 20910
michelle.tomlinson@noaa.gov

Abstract- In this paper, the authors use Spatial Interaction Filters (SIF) to simulate human experts' visual process in tracking spatial interactive objects. The algorithm includes spatial density based pixel clustering and object interaction descriptions, such as Contact Area Index (CAI) and correlation filter. The algorithm is designed to automatically track the Harmful Algae Bloom (HAB) targets. In the case studies, SIF performs well in tracking coherent objects. However, it appears to be weak in tracking the object that breaks into pieces. A comparison between the correlation filter and the particle filter is also presented.

1. INTRODUCTION

Tracking spatiotemporal dynamics of ocean objects, such as harmful algae blooms or river plume, is essential to oceanographic studies. The main functions include: 1) monitoring the movement of an ocean object that has been identified; 2) forecasting the movement of an identified ocean object; 3) predicating conditions favorable for an object to occur where the objects have not been observed. For example, to track and predict an ocean object from a satellite image database, we want to know "where the object goes?" "What are the patterns of movement in the past years?" "Where is the new target?" "In what condition a target would occur?" "What would be the spread pattern if wind speed or direction changed?" To answer those questions, monitoring or tracking an ocean object is fundamental. In this paper, we only focus on tracking Harmful Algae Blooms (HAB). We believe that the same algorithms can be extended for tracking other ocean objects as well.

Remote sensing database, such as SeaWiFS, has been the means for detecting and forecasting the spatiotemporal dynamics of ocean objects. Stedinger and Haddad [32] demonstrated the first use of satellite images for detecting *Karenia brevis* blooms. Stumpf [33] indicated that the use of chlorophyll anomalies can provide a means for monitoring for harmful algal blooms. According to Stumpf's study [18], there is a correlation between chlorophyll and *K. brevis* cell concentration. The relationship appears valid in the field when *K. brevis* dominates phytoplankton species composition, until the concentrations become extremely high. Chlorophyll however is not a reliable indicator for *Karenia*, high chlorophyll is common in many areas without *Karenia*, hence the need for the chlorophyll anomaly technique described in Tomlinson et al. [19] to improve detection and monitoring of these blooms. This method has the added

advantage of clearly showing changes in the chlorophyll field over short time scales.

Unfortunately, ocean object tracking has been done manually, which is expensive and time consuming. For example, to verify a HAB in satellite images normally costs 30 minutes per frame. We still lack general data mining algorithms for automatically monitoring the movement of an ocean object and forecasting the object movement. In particular, there is no available tool to translate scientists' visual knowledge or heuristics into computational languages. In this paper, we intent to develop a computational algorithm that simulate experts' visual process for tracking HAB.

2. PROBLEM

The tracking problem in this study is a two dimensional target detection and morphing process because, from satellite imaging point of view, the ocean objects are visible only at the surface. Given a set of satellite images that contains target areas, where each pixel consists of pixels with coordinates $[x, y]$ and density ρ and noises or artifacts θ at time t , identify target areas (HAB) with distinguishable contour outlines. The number of target areas depends on the predefined level of details.

In this study, the HAB areas can be represented in binary pixels. Tracking the binary pixel targets is not as simple as it appears to be because of the pixel noises, missing data and deformation. Regular tracking algorithms have not been found working properly in this case. For example, Binary Morphology is very vulnerable to the pixel neighborhood and it 'dilates' the targets' shape after a few binary morphological operations. It does not work well when a target has very coarse pixel neighborhood. Furthermore, the spatial density-based clustering algorithms [31] can cluster n -targets in a large database while suppressing pixel noises. However, it does not include target shape information, which is often valuable for determining whether an area is an HAB target or not.

Currently, oceanographic scientists are mainly using visual (manual) method to track the HAB. The manual process appears to be time-consuming, but it does warrant an acceptable accuracy. One of the advantages of the visual tracking process is that humans use multi-dimensional information simultaneously, such as shape and spatial density, multichannel data and historical data. The followings are samples of rules extracted from oceanography scientists:

- *Size*: If the anomaly is too small it is not a HAB.
- *Shape*: If it is a resuspension anomaly it is not a HAB (unless a HAB was previously identified.) If the anomaly extends a long distance along the coast (with coast parallel shape).
- *Region*: If a lump develops in the anomaly field, then it is checked by field data for potential HAB. Check "non-HAB" for chlorophyll lumpiness (areas within the anomaly where the chlorophyll peaks).

To determine the size of an area is straightforward. However, to recognize a shape such as resuspension anomaly, or a track a target that drifts across regions is challenging because this deals with spatial interaction between objects. In this paper, we focus on how to represent those visual heuristics and apply the algorithms to case studies of HAB monitoring.

2. SPATIAL INTERACTION FILTERS

The multi-body interaction dynamics forms visual distributions, shapes, or patterns. The challenge of the visual data mining lies in how to represent a spatiotemporal interaction in a computer. This is involved both cognitive and computational representations. Cognition scientist Leyton [35] developed his theory of shape process grammar that addresses shape deformation dynamics. In his theory, the interactive shapes are classified into extremum types with corresponded process types. On the other side, computer scientists developed clustering models such as spatial density-based models [31] to characterize the pixel 'texture' of an object.

In this paper, we present the Spatial Interaction Filters (SIF) that is to integrate both approaches. The SIF contains models for detecting the contact shape of two objects, tracking correlations of a shape deformation over time, and detecting targeted areas. The SIF contains following filters: 1) multilevel spatial density clustering, 2) spatial correlation and, 3) contact area index. Fig.1 shows an illustration of the SIF model.

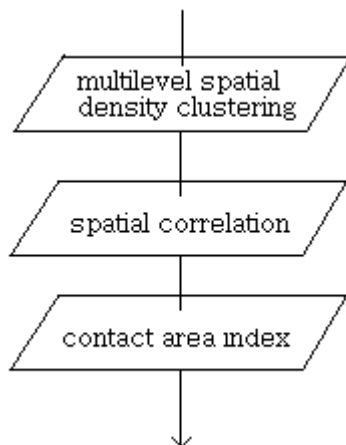


Fig. 1 Spatial Interaction Filters

2.1 Multilevel Spatial Density-Based Clustering

To simplify the spatial object tracking, all the images are converted in binary format. If the RGB value of a pixel exceeds a certain threshold, the value of the corresponding pixel in the resultant images will be 1, otherwise 0. In Fig.2, within a cluster, there are two types of points, core points and non-core points. Core points are those having at least Min of points with the same characteristics within a distance of Dis . This implies the central area of the cluster will have a minimum density of Min / Dis . All the neighboring points within a distance of Dis are classified as the same cluster. Those neighborhoods are then examined to check if they are core points. This process continues recursively. Noises are neither core points nor the neighborhoods of other core points.

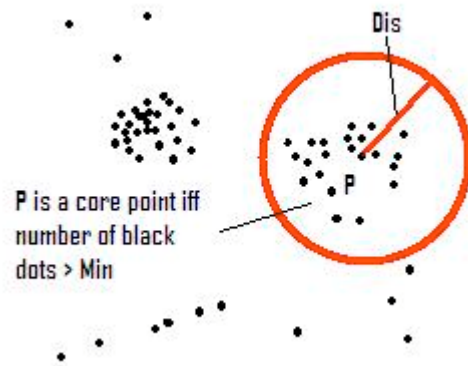


Fig. 2. Spatial Density-Based Clustering

Each pixel of the input image is analogue to a point in database. Each pixel is examined at least once. The only input parameters needed to be determined are Dis and Min . The values for these 2 parameters are rather application-specific. One can tune the values and they can be applied to all the images. The density-based clustering preserves the shape and does not merge those small disconnected blooms to the large ones.

We applied the same clustering algorithm by two passes with two set of values of Dis and Min . The first pass is to remove the noises in the mates and the second one is to filter off small and isolated objects and group the targeted objects together.

For the second pass, we aim at filtering off the small objects which is isolated from the major ones. We chose 40 and 180 for Dis and Min which are large enough to capture those isolated small objects. It is because isolated objects should have much space surrounding it making its density below the threshold. And now a cluster is composed of a number of objects close to each other. It is more like human's eyes that treat a set of disconnected objects close together as a group.

For better visualizing and representing each cluster as a shape, we applied a simplified snake algorithm to find the contour of the cluster. We begin with drawing a minimum

bounding box as the initial contour for each cluster. The coordinates of the box are collected while the clustering algorithm is running. We then shrink the contour by moving its pixel of the contour to the average position of its neighbors. X_{new} and Y_{new} are the new X and Y coordinates of this pixel. X_{left} and X_{right} are the X coordinates of the left pixel and right pixel along the line of the snake. Y_{left} and Y_{right} are similar. α specifies the level of movement of each pixel in each iteration. The quality depends on the number of iterations you want to spend on shrinking the snake. Figure 4 is an example of the output after 5000 iterations. The more iterations the better fit the shape of the anomalies. The only tradeoff is computation time. But the difference is not obvious. Figure 6 also shows the contoured clusters.

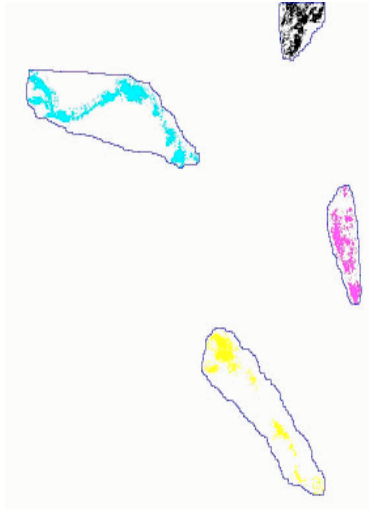


Fig. 3. Active contour sample

2.1 Contact Area Index (CAI Number)

How to describe an object that is in parallel to the contact edge of another object? This is a frequently asked question in oceanography studies. For example, hurricanes cause a lot of resuspension and coastal runoff related with wind and rain. This introduces a lot of suspended solids into the water column. This can be mistaken for newly synthesized chlorophyll. There are two methods to subtract out this resuspension from the chlorophyll anomaly. One way to identify an anomaly is by location and shape. Scientists discovered that if an anomaly extends a distance along the coastline and rather thin in shape, it is likely to be a resuspension event. In another word, resuspension anomalies usually have a shape parallel to the coastline.

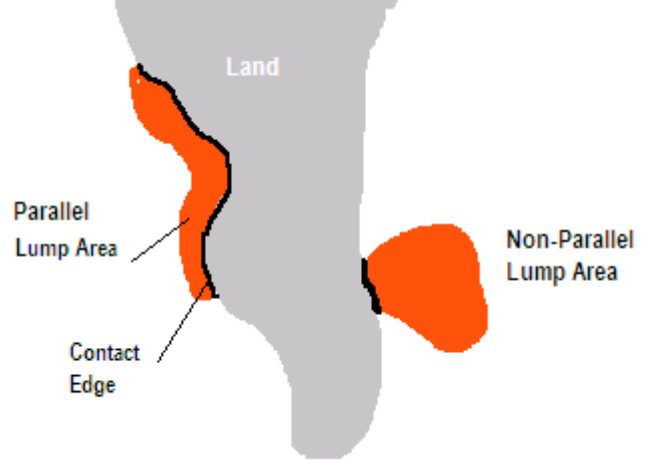


Fig. 4. Contact edge between the bloom and coastline

In an effort to quantifying this observation, Contact Area Index (CAI) is created and is defined as a ratio between the area of object a and the contact length between object a and b . The smaller the CAI number, the more parallelism to the contacted object is. Figure 4 is a visual representation of the calculation of CAI number.

$$CAI = A / L_{ab} \quad (1)$$

where, A is area of the object a , L_{ab} is the length of contacted edge between object a and b .

2.3 Correlation Filter

The matched filter is built by using Fast Fourier Transform and Correlation Theorem:

$$Correlation = IFFT(FFT(a) .* conj(FFT(b))) \quad (2)$$

Where, a is the test image while b is the reference object in the previous image to be tracked. $X = FFT(x)$ and $x = IFFT(X)$ represent Discrete Fast Fourier Transform and Inverse Discrete Fast Fourier Transform respectively.

$$X(k) = \sum_{j=1}^N x(j) \omega_N^{(j-1)(k-1)} \quad (3)$$

$$x(j) = (1/N) \sum_{k=1}^N X(k) \omega_N^{-(j-1)(k-1)} \quad (4)$$

where

$$\omega_N = e^{(-2\pi i)/N}$$

N denotes the length of the vector and symbol $.*$ denotes array multiplication and $conj$ returns the complex conjugate

of the argument. The pixel that gives the highest correlation value has the highest confidence that the reference object is at that pixel location.

3. MONITORING HARMFUL ALGAE BLOOMS

Automatic ocean object tracking requires quantitative analyses of numerous images, specifically, identification of individual blooms. An ability to identify a bloom and then produce an image that codes each bloom uniquely would be quite useful. In the detection and tracking of harmful algae bloom, the Spatial Interaction Filter is mapped into a more application-specific filtering process. Figure 4 shows the process for monitoring harmful algae bloom in an image. Chlorophyll anomaly provides an effective means for monitoring for harmful algae bloom. Stumpf's result shows that chlorophyll anomalies can successfully detect a harmful algae bloom with an accuracy of at 80% in most regions of the Gulf of Mexico. The potential zones are further refined by emulating human's visual analysis. A multi-level density based clustering is applied to the imagery to filter off noises and form clusters of blooms. Contact Area Index (CAI) is used to identify a bloom which has a shape parallel to the eastern coastline of Gulf of Mexico. Any bloom which extends a long distance along the coastline is considered as resuspension event and should be excluded from the analysis. Some regions of the ocean have a very small probability that there is a HAB even if there is a high concentration of chlorophyll anomalies. A bloom developed in a non-HAB region sailed to other part of the ocean is not classified as HAB. Correlation filter is to identify and track the movement of a particular bloom so that blooms developed in the non-HAB region can be filtered.

The pseudo code of the algorithm is as following:

```

Read the raw file of the satellite image
Generate a chlorophyll anomalies image from raw file
Convert the chlorophyll anomalies into binary image
Cluster the binary image to remove noises
Cluster the noise removed binary image to form anomalies groups
For each anomalies group in the current frame
    Compute the Contact Area Index
    If Contact Area Index < threshold
        Remove the group from the chlorophyll anomaly image
    End
End
For each anomalies group LastAnom in the last frame
    Generate a match filter
    Correlate on current frame
    Filter off small correlation value
    For each remaining pixel
        Check if it is the closest to LastAnom
    End
    Find the anomaly group CurrAnom that contains the closest pixel in the
current frame
    If LastAnom is from non-HAB region
        Mark CurrAnom as from non-HAB region
    End
End

```

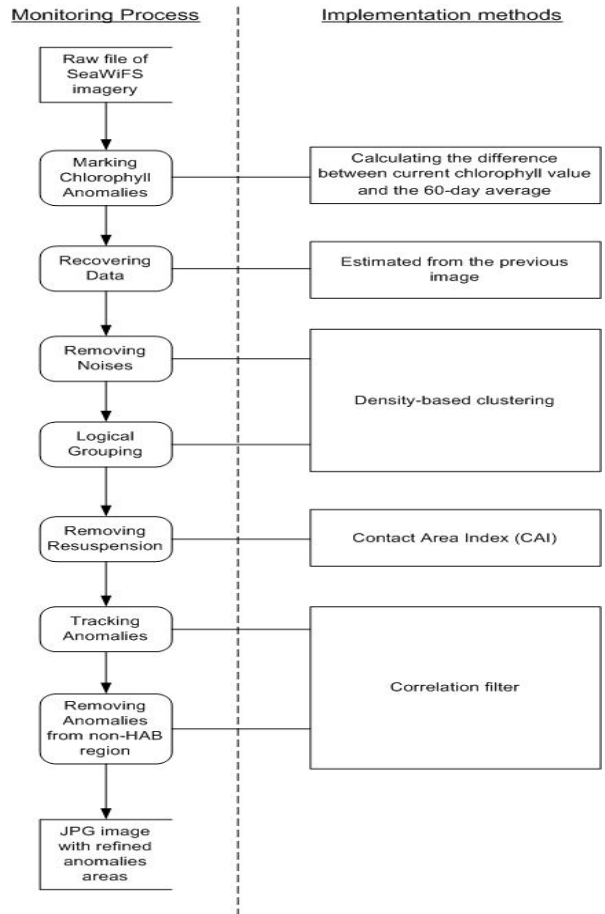


Fig. 4 Block diagram showing the monitoring process

3.1 Data Recovery

HAB has a near linear correlation with the level of Chlorophyll concentration. In practice, scientists use Anomaly images and Chlorophyll images to determine where are the blooms visually. In their experience, Anomaly weighs about 80% and Chlorophyll weighs about 20%. Usually, merely statistical methods do not work because of the noisy data, such as clouds and interference. In this study, we start with simulate expert's visual information process with Artificial Intelligence and Computer Vision algorithms, based realistic data set. Then we move on to find out more suitable mathematical expressions. To simplify the problem, we only use Anomaly images to determine HAB areas, since this approach has at least 80% accuracy.

There are two types of raw data files derived from SeaWiFS database: anomaly files and chlorophyll files. The chlorophyll images contain all eleven channels from the database's original satellite data product. They are band interleaved, with dimensions of 682x730 pixels. We use all 6 reflectances, the albedo, solar zenith angle and landmask in order to throw out pixels which do not meet cloud mask criteria. For example, the land is identified when channel 11 = -1. Clouds are identified by the following: channel9 > (2700 + channel6*0.084). Also, bad pixels are identified

when the solar zenith angle is greater than 60 degrees), therefore, when $\text{channel10} > 600$ (channel ten is equal to satellite zenith angle multiplied by 10). For the anomaly files, values of -32768 refer to bad pixels and clouds.

3.2 Spatial Density-Based Clustering

To simplify the study of HAB, all the chlorophyll anomalies images are represented in binary format. If the RGB value of a pixel exceeds a certain threshold, the value of the corresponding pixel in the resultant images will be 1, otherwise 0. When humans look at a picture or a set of data, their brains will search for the most distinguishable features, ignoring small and evenly distributed objects. During the HAB analysis by oceanographic scientists, they tend to group close but isolated potential anomalies together.

Morphology is a straightforward method in achieving this purpose. It requires the use of a structure element acting as a paintbrush during dilation and erosion. The shapes of the bloom areas are different from the original image depending on the size and shape of the structure element. In order to preserve any information we have, the shape in our case, we treated our image as a small database and applied a density-based database clustering algorithm by Ester, Kriegel, Sander and Xu [31] to remove noise and group the pixels together to emulate the human process.

We start with spatial density clustering because it needs minimal domain knowledge to determine the input parameters and it works with arbitrary shapes. Many existing partitioning algorithms need users to input a parameter k to divide the database into a set of k clusters. As the number of HAB areas varies in each image, we want to have a clustering algorithm that does not need k as input. Also, the shape of a bloom is highly random. It is important to identify the bloom no matter what shape it is.

Within a cluster, there are two types of points, core points and non-core points. Core points are those having at least Min of points with the same characteristics within a distance of Dis . This implies the central area of the cluster will have a minimum density of Min / Dis . All the neighboring points within a distance of Dis are classified as the same cluster. Those neighborhoods are then examined to check if they are core points. This process continues recursively. Noises are neither core points nor the neighborhoods of other core points.

Each pixel of the input image is analogue to a point in database. Each pixel is examined at least once. The only input parameters needed to be determined are Dis and Min . The values for these 2 parameters are rather application-specific. One can tune the values and they can be applied to all the images. Figure 6 and 7 show a comparison between binary morphological processing and density-based clustering algorithm. The density-based clustering preserves the shape and does not merge those small disconnected blooms to the large ones.

From the satellite images, there are some small pixels indicated as bloom in the middle of the ocean which is far

from the coastline. They are obviously not harmful algae bloom. Moreover, scientists are only interested in algae bloom at least of certain size. Therefore, we applied the same clustering algorithm by two passes with two set of values of Dis and Min . The first pass is to remove the noises in the mates and the second one is to filter off small and isolated blooms and group the blooms together.

For the first pass, Dis and Min are 6 and 40 respectively which means a core pixel should have at least 40 other algae bloom pixels within a circle of radius of 6 pixels. The values are chosen in such a way that the circle drawn is just smaller than the smallest bloom that may appear. All the real blooms should have enough density to remain in the image. Each bloom forms a cluster itself.

For the second pass, we aim at filtering off the small blooms which is isolated from the major ones. We chose 40 and 180 for Dis and Min which are large enough to capture those isolated small blooms. It is because isolated blooms should have much space surrounding it making its density below the threshold. And now a cluster is composed of a number of blooms close to each other. It is more like human's eyes that treat a set of disconnected objects close together as a group. Figure 6 shows the result after the second pass. Without the first pass, some noises which are close to those large blooms will be captured.

For better visualizing and representing each cluster as a shape, we applied an active contour model to find the outline of the cluster. We begin with drawing a minimum



Fig. 5. Noise filtered by the first pass of the clustering algorithm

bounding box as the initial contour for each cluster. The coordinates of the box are collected while the clustering algorithm is running. We then shrink the contour by moving its pixel of the contour to the average position of its

neighbors. CAI numbers are then calculated between each contoured cluster and the coastline of the Gulf of Mexico. If any contoured cluster falls below the threshold, it is marked as potential resuspension. Experiments show that resuspension usually has a CAI number less than 70. Figure 6 shows the sample values of CAI number.

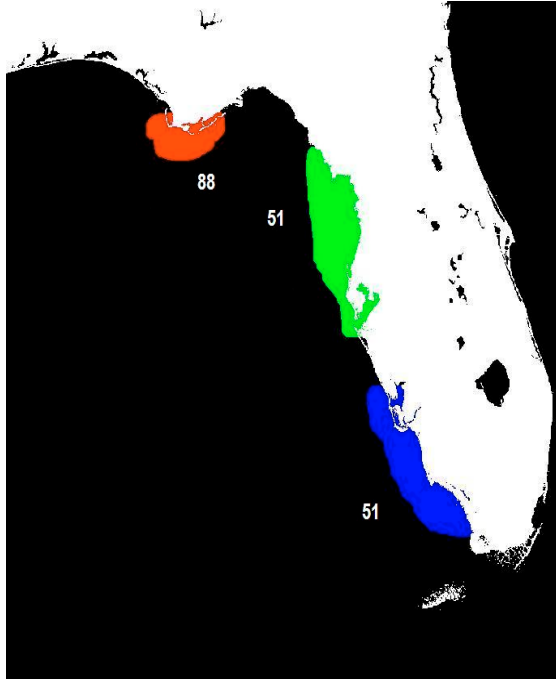


Fig. 6. Samples of Contact Area Index

3.3 Correlation Filtering

The chlorophyll anomalies may capture different kinds of blooms and only some of them are harmful. A region of the Gulf of Mexico is suggested that it is impossible to distinguish harmful blooms from the anomalies due to the optical complexity of the region. Historical data also shows that harmful algae blooms are infrequent in this region. Therefore, we assume that any anomaly developed in this region is not HAB. However, non-HAB may move to other regions of the coastline. It is necessary to track if an anomaly in a HAB region is actually coming from a non-HAB region. HAB recognition and tracking is done by correlation filter on each image frame.

The consecutive images may show a large difference because the time elapsed between each image varies. The shape of the bloom may change dramatically and there may be more than one peak value. In this case, the peak that is closer to the center of the reference object will be picked. If there exists more than one cluster in the location of the reference object, the reference object is considered as breaking into pieces. The process continues by using the newly identified anomaly as the reference object for the next

image frame. Figure 9 shows the tracking of a particular anomaly.

4. RESULTS

We used the dataset of the east coastline of the Gulf of Mexico from NOAA to test the HAB monitoring. After a series of filters applied onto the image, Figure 7 and 8 show the chlorophyll anomalies image before and after processing respectively. Figure 9 shows the sample output of the tracking.

To provide a benchmark for our tracking performance, we compared our results with that of particle filters, which is an inference technique for estimating unknown motion state from a noisy collection observation over time. To be more specific, it is to approximate the posterior distribution by a set of weighted particles with respect to the adaptive model. More details can be found in [35].

Figure 10 shows a result from the particle filter. Table 1 shows the acceptable percentage of both SIF with correlation filter and particle filter. The result is considered as an acceptable if and only if the box is bounding the expected target. SIF achieved 95% on tracking performance on this dataset while particle filter yielded 50%.

We have shown results using our Spatial Interaction Filter approach for tracking the movement and deformation of chlorophyll anomalies and compared it to the particle filter with appearance adaptive model. By comparing Figure 9 and 10, first, we can see that SIF has a higher accuracy in indicating the whole tracking object, i.e. the whole object is highlighted. For particle filter, the box is loosely bounded and some part of the target is outside of the box. The boxes in Figure 9 are added manually for better illustration in black and white images. Particle filter only outputs the boxes as shown in Figure 10. Second, particle filter cannot continue tracking correctly once the target has moved significantly. In our experiment, there is a large variation between image 40 and 41. Particle filter lost its target and produced wrong result for the rest of 39 images. In general, particle filter works well if the image frames shows smooth changes but it is not necessarily true in our application. In addition, SIF with correlation filter has better tolerance to abrupt movement.

We also tested some extreme cases, e.g. the bloom breaks into two pieces. The experiment is repeated again by using the same set of images but the target bloom is changed. This bloom extends a longer distance along the coastline than the previous one. Starting from image 21, the bloom broke into 2 pieces. SIF with correlation filter continued tracking for the smaller piece only but particle filter still captured both of them. At the later stage of the tracking, SIF only track one of the pieces. Figure 11 and 12 show the results for both approaches. We believe we can add more rules to accommodate the splitting in the near future. Moreover, after using the density-based clustering, pixels are no longer independent and we are able to highlight the whole anomalies.

Table 1. SIF with Correlation Filter versus Particle Filter

Method	SIF with Correlation Filter	Particle Filter
acceptable % for Case 1 (target totally located)	79/79 = 100%	40/79 = 50%
acceptable % for Case 2 (split to two pieces)	48/79 = 60%	79/79 = 100%

5. CONCLUSIONS

Spatial Interaction Filters (SIF) is aimed to simulate human experts' visual process in tracking spatial interactive objects. The algorithm includes spatial density based pixel clustering, and object interaction descriptions, such as Contact Area Index (CAI) and correlation matching. The results show that the model can remove the artifacts, determine the resuspension by shape, and track the selected target area.

In our test cases, we found SIF performs well in tracking a HAB with tolerance to abrupt movement and SIF gives accurate outline of the tracked areas. However, it appears to be weak in tracking the shape that breaks into pieces. Our future work includes the study of how to make a more robust model for monitoring HAB in larger data sets.

ACKNOWLEDGMENTS

Our thanks to NASA Grant AIST-QRS-04-3031 and Dr. Gene Carl Feldman, SeaWiFS program manager and Dr. Horace Mitchell, Director of Scientific Visualization Studio, NASA GSFC, for their support.

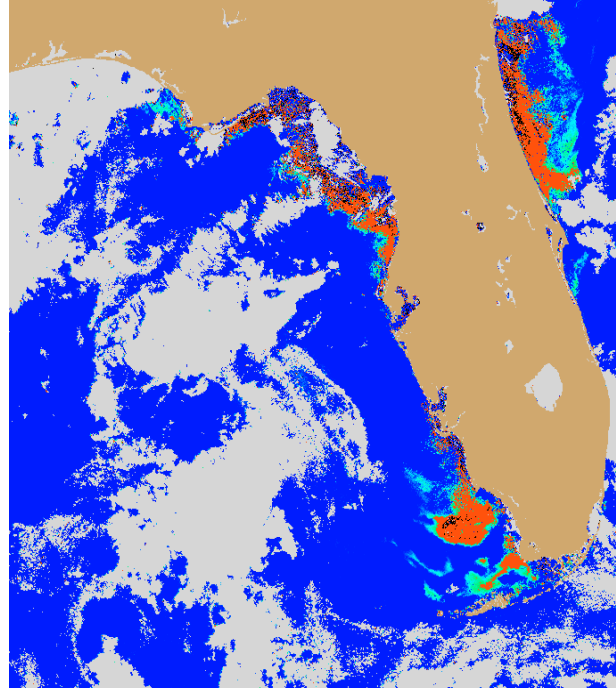


Fig. 7. Satellite image before processing

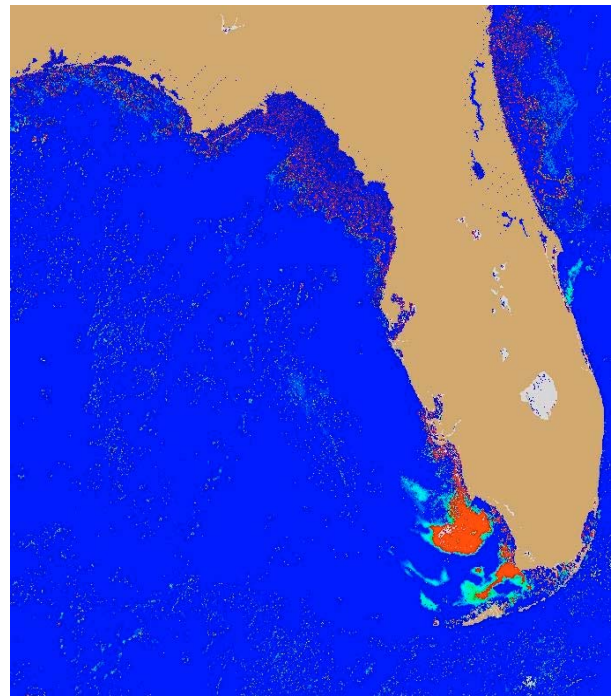


Fig. 8. Satellite image after processing

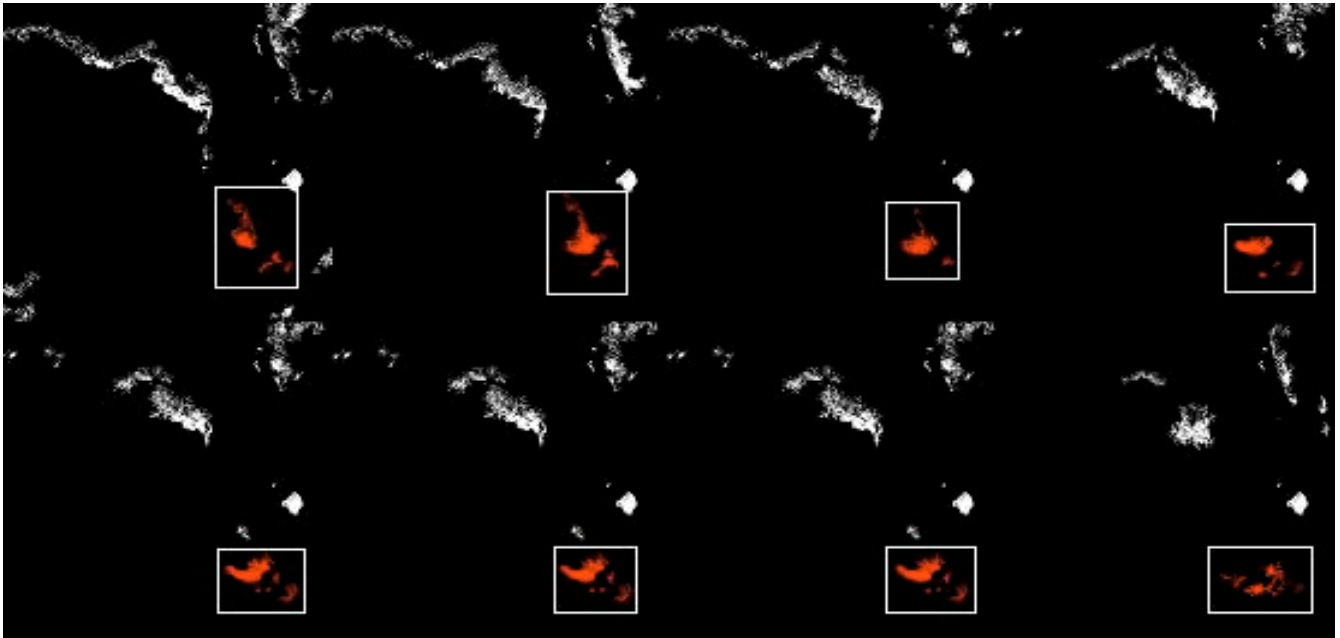


Fig. 9. Tracking of a bloom which has moved significantly sampled in an interval of 4 days using SIF

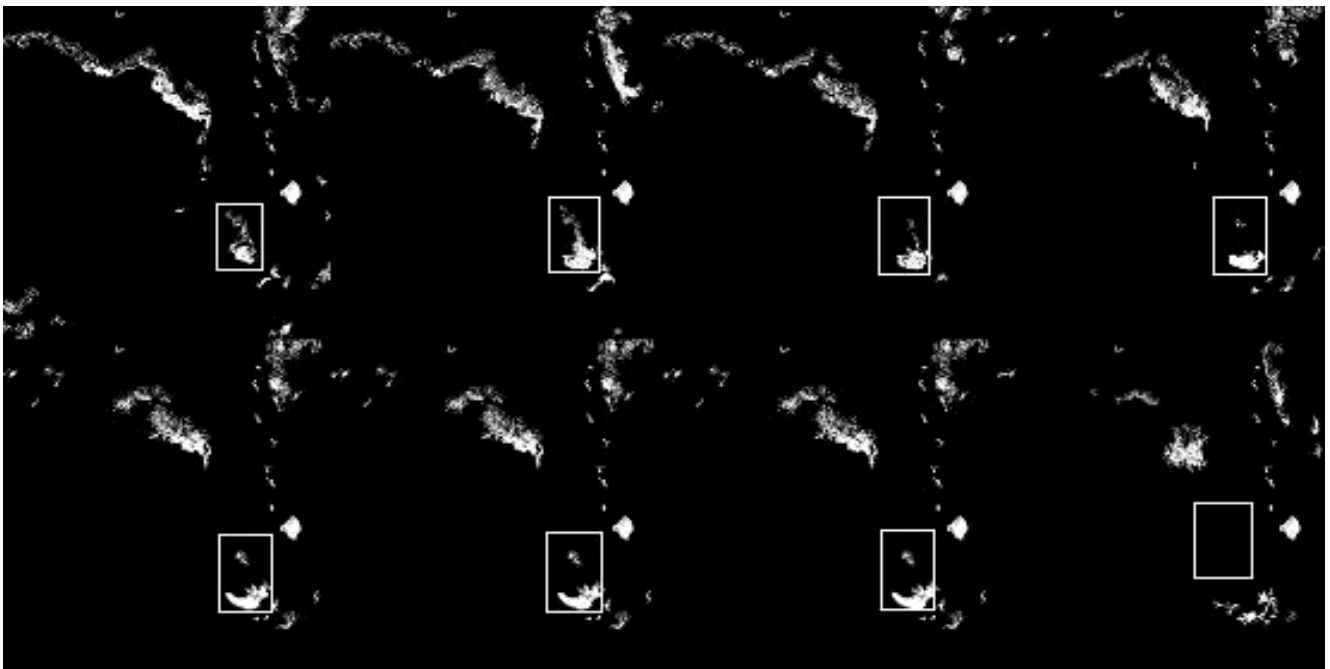


Fig. 10. Tracking of a bloom which has moved significantly sampled in an interval of 4 days using particle filter

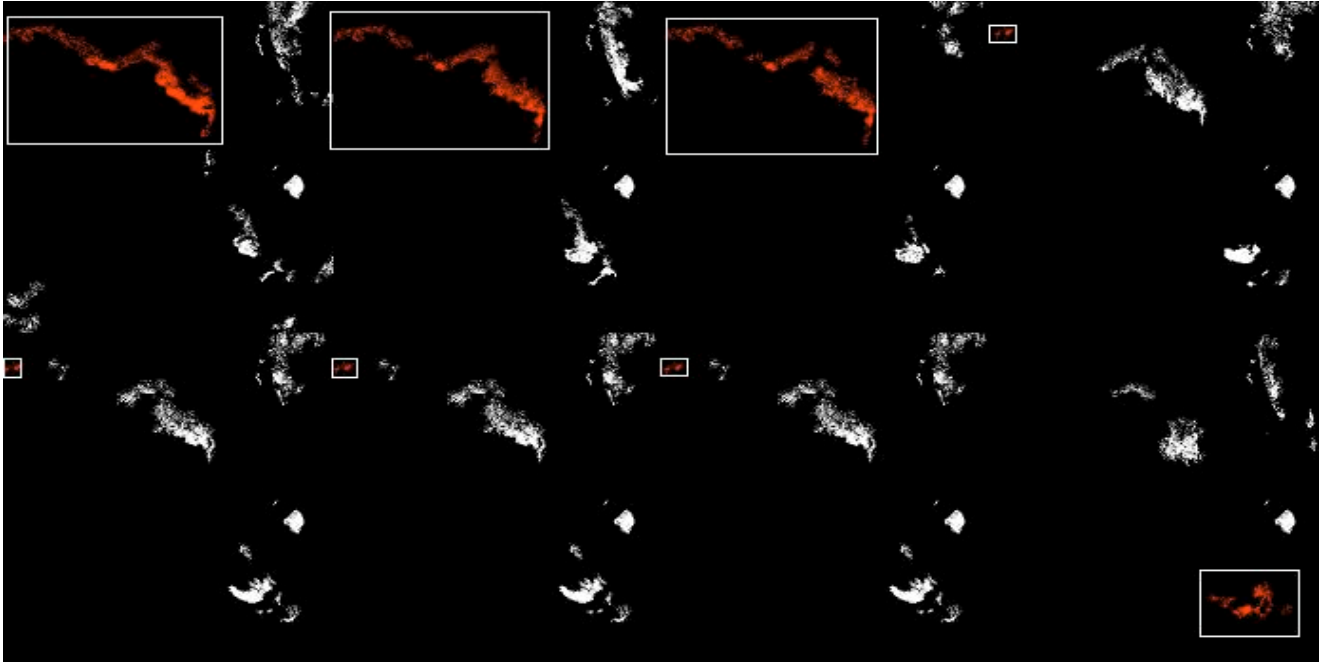


Fig. 11. Tracking of a bloom which has split into 2 pieces sampled in an interval of 4 days using SIF

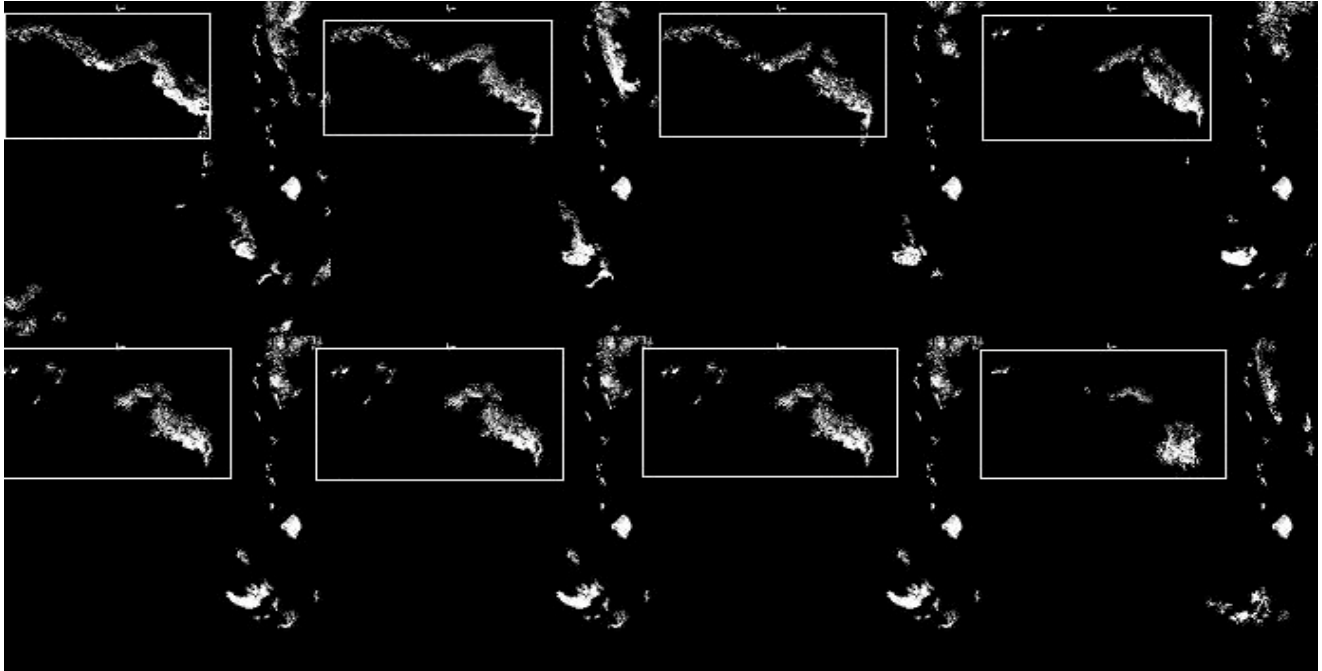


Fig. 12. Tracking of a bloom which has split into 2 pieces sampled in an interval of 4 days using particle filter

REFERENCES

- [1] Bowman, B., Debray, S. K., and Peterson, L. L. Reasoning about naming systems. *ACM Trans. Program. Lang. Syst.*, 15, 5 (Nov. 1993), 795-825.
- [2] Chen, X., S.E. Lohrenz, D.A. Wiesenburg, 2000. Distribution and controlling mechanisms of primary production on the Louisiana-Texas continental shelf. *Journal of Marine Systems*, 25: 179-207.
- [3] Doney, S.C., R. Anderson, J. Bishop, K. Caldeira, C. Carlson, M.-E. Carr, R. Feely, M. Hood, C. Hopkinson, R. Jahnke, D. Karl, J. Kleypas, C. Lee, R. Letelier, C. McClain, C. Sabine, J. Sarmiento, B. Stephens, and R. Weller, 2004: Ocean Carbon and Climate Change (OCCC): An Implementation Strategy for U. S. Ocean Carbon Cycle Science, UCAR, Boulder, CO, 108pp. <http://www.carboncyclescience.gov/occc-report.html>
- [4] Framinan, M.B. and O.B. Brown, 1996. Study of the Rio de la Plata turbidity front, Part I: spatial and temporal distribution. *Continental Shelf Research*, 16(10): 1259-1282.
- [5] Gilbes, F., F.E. Muller-Karger, C.E. Del Castillo, 2002. New evidence for the West Florida Shelf Plume. *Continental Shelf Research*, 22: 2479-2496.
- [6] McClain, C.R., J.A. Yoder, L.P. Atkinson, J.O. Blanton, T.N. Lee, J.J. Singer, F. Muller-Karger, 1988. Variability of surface pigment concentrations in the South Atlantic Bight. *Journal of Geophysical Research*, 93: 10,675-10,697.
- [7] Tomlinson, M.C., R.P. Stumpf, V. Ransibrahmanakul, E.W. Truby, G.J. Kirkpatrick, B.A. Pederson, G.A. Vargo, C. A. Heil., 2004. Evaluation of the use of SeaWiFS imagery for detecting *Karenia brevis* harmful algal blooms in the eastern Gulf of Mexico. *Remote Sensing of Environment*, v. 91, pp. 293-303.
- [8] Salisbury, J.E., J.W. Campbell, L.D. Meeker, C. Vorosmarty, 2001. Ocean color and river data reveal fluvial influence in coastal waters. *EOS, Transactions, American Geophysical Union*, 82(20): 221, 226, 227.
- [9] Stumpf, R.P., 1988. Sediment transport in Chesapeake Bay during floods: analysis using satellite and surface observations. *Journal of Coastal Research*, v. 4 p. 1-15.
- [10] Stumpf, R.P., G. Gelfenbaum, and J.R. Pennock, 1993. Wind and tidal forcing of a buoyant plume, Mobile Bay, Alabama. *Continental Shelf Research*, v. 13(11), p. 1281-1301.
- [11] Stumpf, R.P. and P. Goldschmidt, 1992. Remote sensing of suspended sediment discharge in the western Gulf of Maine, April 1987 100-year flood. *Journal of Coastal Research*, v. 8, p. 218-225.
- [12] Crutchfield J. P., Kaneko K., 1987, "Phenomenology of Spatio-Temporal Chaos," in Bai-lin H. (ed.), *Directions in Chaos*, Singapore, World Scientific.
- [13] Kirkpatrick S., Gelatt C., Vecchi M., 1983, "Optimization by Simulated Annealing" *Science* **220** 671-680
- [14] Semboloni F., 1999, "A Coupled map lattice approach to the simulation of land-use and transportation. Case Study of Abidjan" in P. Rizzi (ed.) *Computers in Urban Planning and in Urban Management on the Edge of the Millennium*, Milano, F. Angeli.
- [15] Tobler W. R., 1970, "A computer movie simulating urban growth in the Detroit region," *Economic Geography*, **46**, 234-240.
- [16] White R., Engelen G., Uljee I., 1997, "The use of constrained cellular automata for high-resolution modelling of urban land-use dynamics," *Environment and Planning B: Planning and Design*, **24**, 323-343.
- [17] Walker, N.D. 1996. Satellite assessment of Mississippi River plume variability: causes and predictability. *Remote Sensing of Environment*, 58: 21-35.
- [18] Stumpf, R.P., M.E. Culver, P.A. Tester, M. Tomlinson, G.J. Kirkpatrick, B.A. Pederson, E. Truby, Ransibrahmanakul, M. Soracco, Monitoring *Karenia brevis* blooms in the gulf of Mexico using satellite ocean color imagery and other data, *Harmful Algae* 2(2003) 147-160
- [19] Tomlinson, M., R.P. Stumpf, V. Ransibrahmanakul, E.W. Truby, G.J. Kirkpatrick, B.A. Pederson, G.A. Vargo, C.A. Heil. Evaluation of the use of SeaWiFS imagery for detecting *Karenia brevis* harmful algae blooms in the eastern Gulf of Mexico, *Remote Sensing of Environment*, 91(2004) 293-303
- [20] Serra, J.: *Image analysis and mathematical morphology*. Orlando, San Diego, San Francisco, New York, London, Toronto, Montreal, Sydney, Tokyo: Academic Press 1982
- [21] Serra, J.: *Image analysis and mathematical morphology, Volume 2: Theoretical advances*. Orlando, San Diego, San Francisco, New York, London, Toronto, Montreal, Sydney, Tokyo: Academic Press 1982
- [22] Huppert, A., Blasius, B., and Stone, L. A model of Phytoplankton blooms, *The American Naturalist*, vol. 159, no. 2, Feb. 2002
- [23] Matsunashi, S., S. Inoba, H. Shimogaki and Y. Miyanaga, Water Quality Simulation and Analysis of Blue Green Algae Growth Limiting Factor in Lake Teganuma, online archive.
- [24] MacCready, P. Numerical circulation modeling as a tool for Harmful Algae Bloom research and prediction, online archive. www.ocean.washington.edu/people/faculty/parker/hab's_in_puget_sound.htm
- [25] Franks, P.J.S. 1997. Spatial patterns in dense algae blooms, *Limnol. Oceanography*. 42: 1297-1305.
- [26] Anderson, D.M. 1997. Bloom dynamics of the toxic *Alexandrium* species in the northeastern U.S. *Limnol. Oceanogr.* 42:1009-1022.
- [27] Steidinger, K.A.. 1975. Basic factors influencing red tides. *Proceedings of the First International Conference on Toxic Dinoflagellate Blooms*, V.R. LoCicero (ed), pp. 153-159.
- [28] About DeciDe-HAB, www.nrsc.no/HAB/about.htm
- [29] About HABs Fuzzy Logic, www.habes.net/about/fuzzy_logic.htm
- [30] Runsick, C. Mending Holes in the Ocean's Food Web, www.ovpr.uga.edu/researchnews/93sp/ocean.html
- [31] M. Ester, H Kriegel, J. Sander, X. Xu. A Density-Based Algorithm for Discovering Clusters in Large Spatial Databases with Noise. In Evangelos Simoudis, Jiawei Han, and Usama M. Fayyad, editors, *Proceedings of the Second International Conference on Knowledge Discovery and Data Mining (KDD-96)*. AAAI Press, 1996, pp. 226-231.
- [32] Stedinger, K.A., & Haddad, K. Biologic and hydrographic aspects of red tides. *Bioscience*, 31(11), 814-819
- [33] Stumpf, R.P.: Applications of satellite ocean color sensors for monitoring and predicting harmful algae blooms, *Hum. Ecol. Risk Assess.* 7(5), 1363-1368
- [34] Leyton, M.: "Shape as Memory Storage," in Yang Cai (ed), "Ambient Intelligence for Scientific Discovery," *Lecture Notes in Artificial Intelligence (LNAI)*, Volume 3345, Springer, 2005
- [35] Zhou, S.K. Chellappa, R. and Moghaddam, B.: "Visual Tracking and Recognition Using Appearance-Adaptive Models in Particle Filters, *IEEE Trans. On Image Processing*, Vol. 13, No. 11, November 2004